ELSEVIER

Journal of Alloys and Compounds 434–435 (2007) 319–323

Journal of ALLOYS AND COMPOUNDS

www.elsevier.com/locate/jallcom

Quasicrystal phase formation in Al–Cu–Fe nanopowders during field-activated sintering (FAST)

R. Nicula[a,*], F. Turquier[a], M. Stir[a], V.Y. Kodash[b], J.R. Groza[b], E. Burkel[a]

[a] *Institute of Physics, Rostock University, August-Bebel-Strasse 55, D-18055 Rostock, Germany*
[b] *Chemical Engineering Materials Science Department, University of California at Davis, CA 95616, USA*

Abstract

The sequence of solid-state phase transformations in high-energy ball-milled Al–Cu–Fe alloy powders upon constant-rate heating were examined by *in situ* synchrotron radiation diffraction and thermal analysis (DSC/DTA) methods. The as-milled Al–Cu–Fe nanopowders were consolidated into disk-shape pellets using field-activated spark-plasma sintering (FAST/SPS). The chemical homogeneity and microstructure of the sintered bodies were investigated using scanning electron microscopy (SEM/EDX). The effect of electric field application on the formation of quasicrystalline phases from mechanically activated nanopowders during sintering by FAST/SPS is discussed.

Keywords: Quasicrystals; Sintering; Powder metallurgy; Mechanical alloying

1. Introduction

Due to their unique aperiodic long-range atomic order, quasicrystals (QC's) exhibit a broad variety of physical, chemical, mechanical and tribological properties unusual for metallic systems [1,2]. Quasicrystal-forming alloys consequently hold a high potential for applications like high-temperature thermal barriers, low-friction and wear-resistant coatings [1-3], composite biomaterials [4] or catalysts [5]. The synthesis of single-phase Al–Cu–Fe QC's by conventional casting is nevertheless difficult, due to their very narrow composition domain [6]. Recent research efforts were devoted to the mechanosynthesis of quasicrystalline Al–Cu–Fe powders by powder metallurgy (P/M) routes [7–10] and their pressure- or field-assisted consolidation [11]. The influence of external pressure onto the sequence of solid-state interdiffusion reactions leading to single-phase Al–Cu–Fe QC's was evaluated in a recent paper [12]. The main aim of the present work is to investigate the formation of icosahedral (iQC) phases and related complex metallic alloys under pulsed current application. The effect of fast heating and of electric field application on the formation of QC's during the rapid consolidation of ball-milled Al–Cu–Fe powders by field-activated spark-plasma sintering (FAST/SPS) are assesed by comparison with ambient pressure non-isothermal sintering at low heating rates.

2. Experimental

Nanocrystalline (nc-) Al–Cu–Fe powders were prepared by mechanical alloying (MA). Wet-milling in hexane was employed to counteract severe powder losses during MA [10,11], avoid severe contamination from grinding media and prevent oxidation effects. No other milling additives were used. High purity powders of Al (99.95%), Cu (99.95%) and Fe (99.95%) were loaded into 250 ml hardened chromium–steel vials together with 10 and 20 mm steel balls. The ball-to-powder ratio (BPR) was chosen approximately equal to ≈14:1.

The formation of QC's during non-isothermal annealing of the Al–Cu–Fe nanopowders was studied by differential scanning calorimetry and high-temperature synchrotron radiation diffraction (HTXRD). In-situ experiments were performed at the B2 high-resolution diffraction beamline [13] of HASYLAB (Hamburg). The XRD patterns were collected each 25 °C during constant-rate heating at 2.5 °C/min.

Field-activated sintering (FAST) was performed using a spark-plasma sintering SPS machine (Sumitomo, Japan) with pulsed DC voltage (2–4 V; pulse cycle: 12 pulses ON/2 pulses OFF, pulse duration 3 ms). The Al–Cu–Fe nanopowders were loaded into graphite die-punch units to sinter disc-shaped pellets of about 20 mm diameter. The FAST/SPS experiments were conducted in vacuum, under an applied uniaxial pressure of 55 MPa.

3. Results

Al–Cu–Fe allloy nanopowders with particle sizes between 5 and 20 μm and average crystallite size close to 10 nm were obtained after wet-milling in hexane for 40 h at 200 rotations per

---

[*] Corresponding author. Tel.: +49 381 498 6869; fax: +49 381 498 6862.
E-mail address: nicula@physik1.uni-rostock.de (R. Nicula).

0925-8388/$ – see front matter © 2006 Elsevier B.V. All rights reserved.
doi:10.1016/j.jallcom.2006.08.195

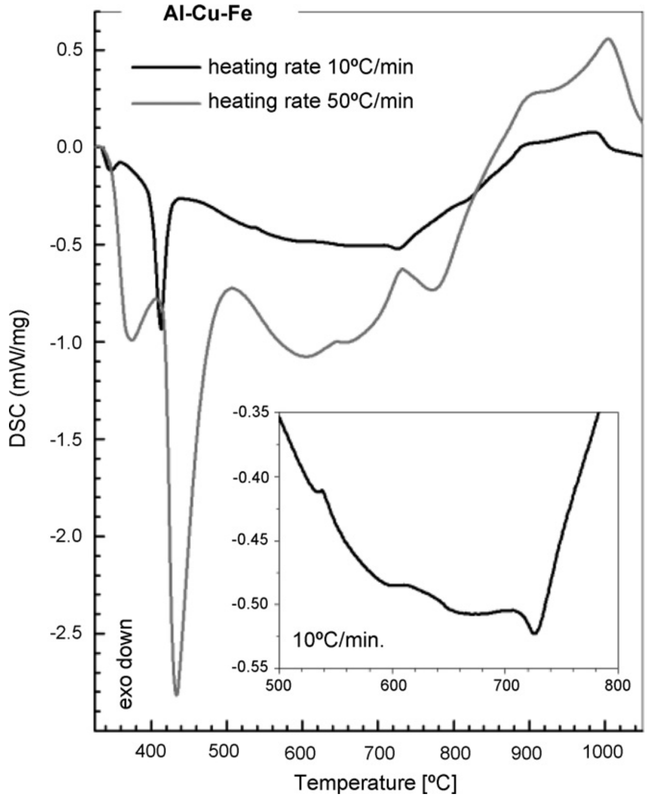

Fig. 1. DSC traces of Al–Cu–Fe nanopowders at heating rates equal to 10 and 50 °C/min.

minute. The X-ray diffraction patterns of the as-milled powders indicate the formation of bcc β-Al(Cu,Fe) and tetragonal θ-Al_2Cu phases. The chemical composition of as-milled powders equals $Al_{65}Cu_{23}Fe_{12}$ as shown by scanning electron microscopy (SEM/EDX).

The thermal behaviour during non-isothermal heating was studied by differential scanning calorimetry (DSC) performed for several heating rates up to 50 °C/min. The DSC traces obtained during heating at 10 and 50 °C/min. are shown in Fig. 1. Two well-defined exothermal events are clearly distinguished in the low temperature range below 500 °C, presumably related to the formation of $AlFe_3$ and Al_7Cu_2Fe phases. A more complex sequence of thermal events is observed above 500 °C. The increase of the heating rate causes a moderate shift (∼20 °C) of the phase transition temperatures towards higher values, otherwise the sequence of thermal events does not change.

The high-resolution HTXRD patterns of the nc-AlCuFe powders during constant-rate heating at 2.5 °C/min. are shown in Fig. 2. The phase constitution of the Al–Cu–Fe alloy changes several times upon heating: the *in situ* synchrotron radiation diffraction experiment reveals a significant overlapping of the thermal stability fields of the constituent alloy phases.

Selected diffraction patterns at different temperatures are also shown (Fig. 3), to illustrate in more detail the solid-state transformation path. The as-milled powders consist of β-Al(Cu,Fe) and θ-Al_2Cu phases. The presence of Al_2Cu and Fe_3Al phases at lower temperatures is mainly due to the positive heat of mixing (15 kJ/mol) of the Fe–Cu pair [7,9].

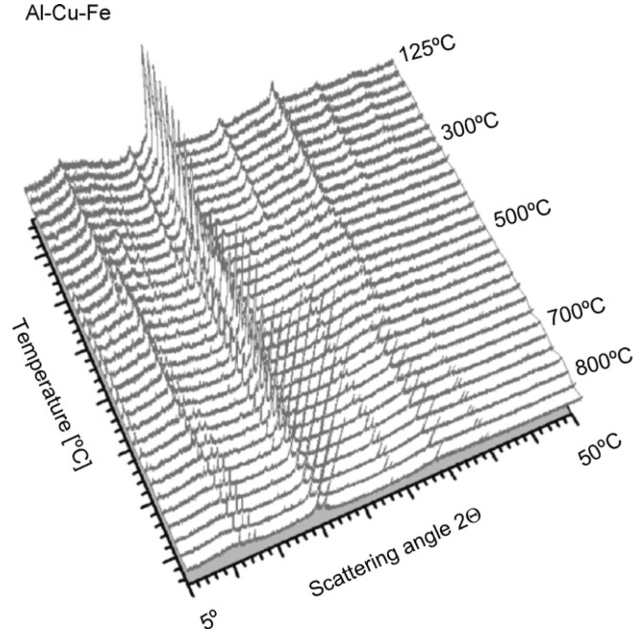

Fig. 2. *In situ* high-temperature diffraction (HTXRD) patterns of nanocrystalline Al–Cu–Fe alloy powders.

The formation of the iQC ψ-phase during non-isothermal annealing is found to occur according to the following sequence of phase transitions:

$$\begin{aligned}&\beta\text{-Al(Cu, Fe)} + \theta\text{-}Al_2Cu(+Al) \rightarrow \beta + \theta + Fe_3Al\\&\rightarrow \theta + Fe_3Al + \omega\text{-}Al_7Cu_2Fe\\&\rightarrow \omega(+Fe_3Al) \rightarrow \omega + \psi \rightarrow \psi\end{aligned}$$

in good agreement with other literature results [7]. The corresponding constituent phase stability fields were also determined (Fig. 4).

The ω-Al_7Cu_2Fe phase is the main precursor of the iQC ψ-phase. As the homogenization of the alloy composition is gradually completed, the ω-Al_7Cu_2Fe becomes the major constituent phase. Minor traces of Fe_3Al were still noticed in the XRD patterns after the nucleation of the iQC phase at approximately 600 °C. The metastable bcc γ-phase (Al_4Cu_9-type) was not detected. The F-type iQC ψ-phase forms via the ordering of the ω-Al_7Cu_2Fe intermetallic and develops into a single-phase above 750 °C (Fig. 3). The quasilattice parameter of the ψ-phase at 800 °C was found equal to $a_q = 0.4516$ nm. The average crystallite size (Scherrer equation) of the ψ-phase is 0.12 μm.

The as-milled Al–Cu–Fe powders were FAST sintered for 20 min at 700 °C to obtain disk-shaped bulk pellets with a thickness of about 2.8 mm. A typical FAST sintering diagram is shown in Fig. 5. During the initial stage, the nc-AlCuFe powders are heated to 700 °C at 40 °C/min. The isothermal stage is defined by a dwell time of 20 min at the sintering temperature (700 °C). The final specimen cooling stage occurs in two steps: a faster cooling at 25 °C/min. under pulsed current application, followed by very slow cooling under uniaxial pressure without field application.

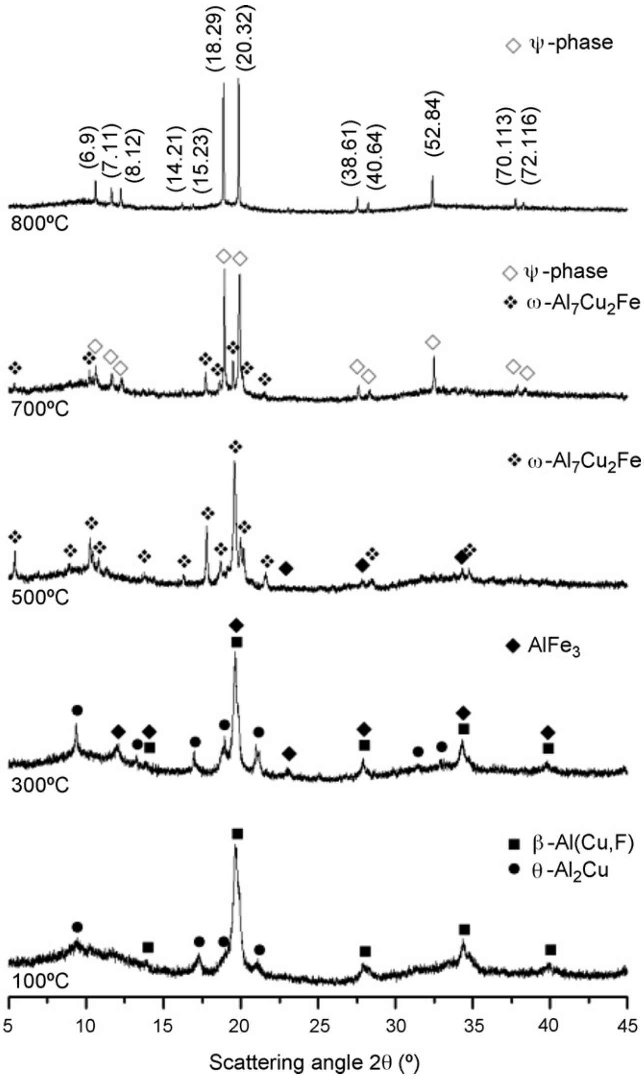

Fig. 3. Selected XRD patterns collected during *in situ* constant rate heating of nc-AlCuFe showing the phase evolution towards the formation single-phase quasicrystals above 750 °C.

The displacement rate of the upper die (signal (2), Fig. 5) monitors the densification of the powder specimen. It is seen that densification occurs mainly during the initial heating stage of the FAST process and less during the isothermal holding at the sintering temperature (700 °C). Hence shortening of the isothermal stage would prevent excessive grain-growth and significantly shorten the FAST process. This result further points out the need for a detailed examination of the microstructural evolution, and of the formation and stability of constituent phases during non-isothermal heat treatments. Thermal analysis coupled to *in situ* synchrotron radiation diffraction experiments are ideal tools to accomplish this task.

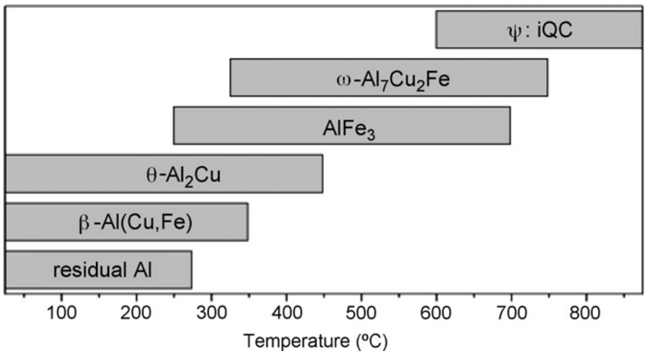

Fig. 4. Temperature evolution of the alloy phase constitution for nc-AlCuFe powders upon constant rate heating.

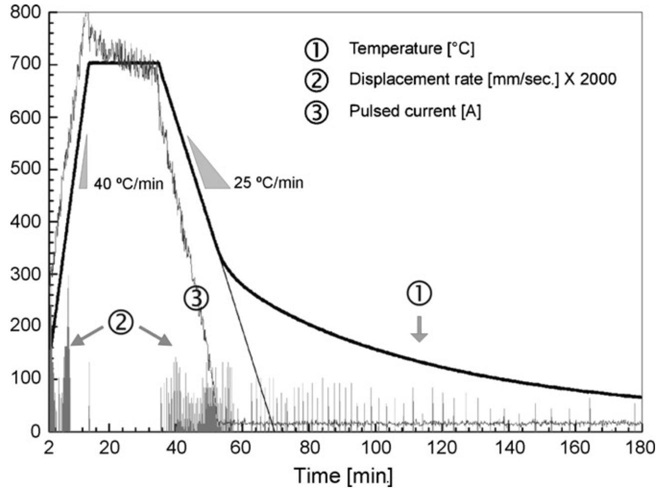

Fig. 5. Typical FAST-SPS sintering diagram: (1) temperature, (2) displacement rate (in mm/s), (3) pulsed current.

SEM micrographs of the cross-section (fracture surface) of the sintered pellets indicate that fairly uniform, ultrafine microstructures were preserved throughout the specimen thickness during processing by FAST. Neither large pore agglomerates, exaggerated grain-growth nor macroscopic defects such as cracks are noticed. The SEM micrographs (Fig. 6) reveal that the fine scale of the as-milled powders is not altered during FAST.

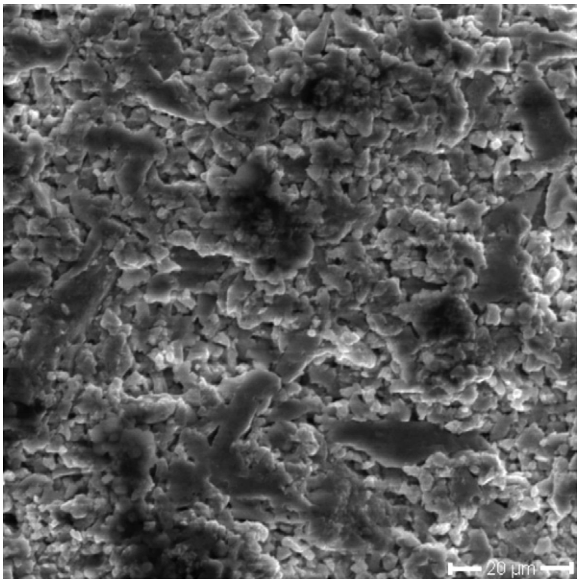

Fig. 6. SEM micrograph of the fracture surface of the AlCuFe FAST-sintered specimen.

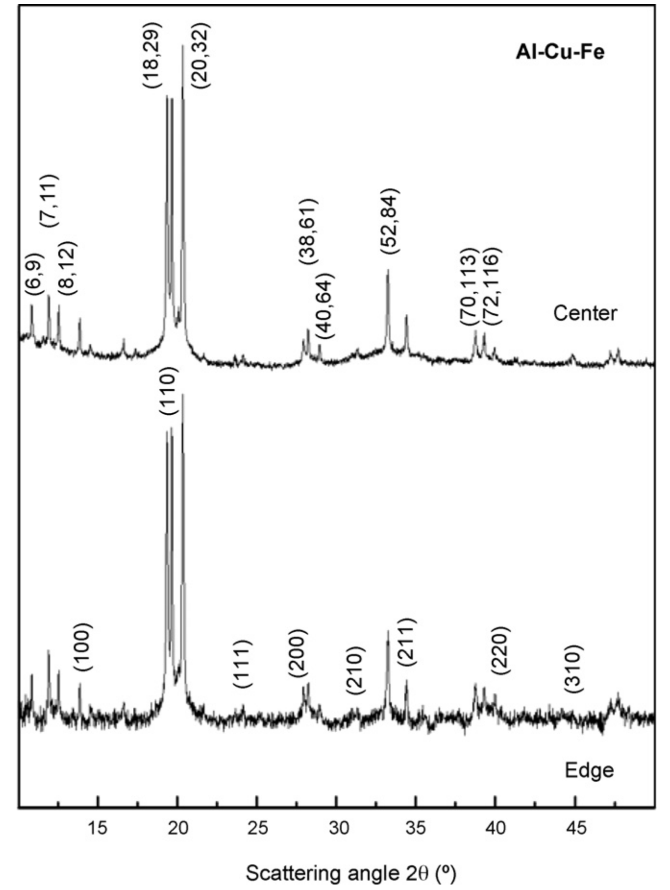

Fig. 7. XRD patterns obtained from the centre and near edge region of a FAST sintered pellet.

This is mainly due to the limited exposure to high temperatures. The observed morphology of the FAST sintered pellets is reminiscent of interlocked microstructures, likely to form upon (partial) melting. Interlocked microstructures are known to assist the general improvement of mechanical properties (toughness) of the FAST sintered parts [14].

The sintered specimens still exhibit uniform porosity in the submicron range. An uniform distribution of small pores was shown to be a prerequisite for the suppresion of pore coarsening [15] and thus also for obtaining full-density sintered parts.

X-ray microdiffraction was employed to investigate the uniformity of the sintered parts. Synchrotron radiation diffraction patterns were collected from the outer surfaces of the pellets. The diffraction patterns taken from the centre and specimen edge are identical (Fig. 7). The sintered parts consist of bcc β-Al(Cu,Fe) and iQC ψ-phases: the β-phase is indexed by (*h k l*) Miller indices (bottom), the ψ-phase using Cahn (*N*, *M*) indices (Fig. 7).

Chemical mapping by SEM/EDX further confirmed the high homogeneity of the sintered pellets (Fig. 8). We may thus conclude that either an uniform thermal field was applied throughout the volume of the bulk sintered body during FAST processing or that thermal gradients did not affect the phase structure of the specimens. Rapid densification is achieved without alteration of the initial ultrafine microstructure of the starting powders. The bulk sintered parts consist of a fine mixture of iQC ψ-phase and bcc β-Al(Cu,Fe).

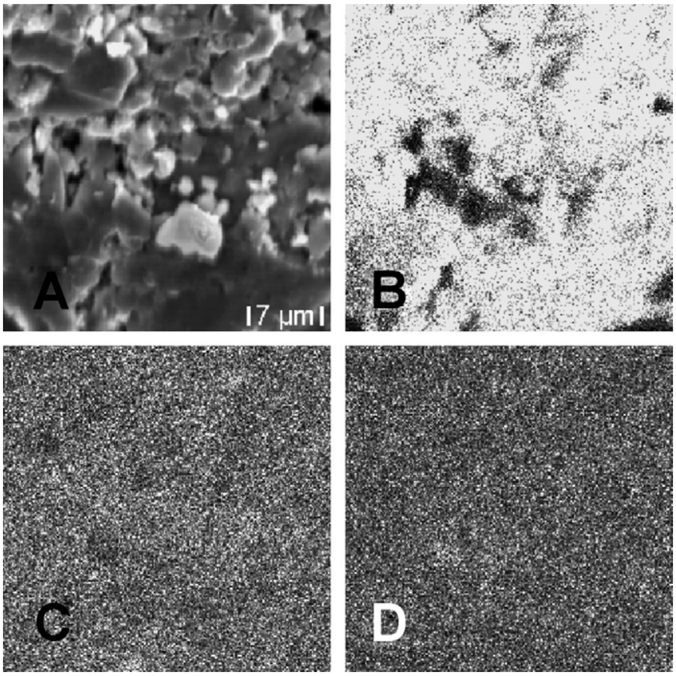

Fig. 8. EDX composition maps of the region A (bright image), showing the spatial distribution of Al (B), Cu (C) and Fe (D).

4. Discussion and conclusions

Nanocrystalline powders were obtained by ball-millling of pure elemental powders in liquid media. Single-phase quasicrystalline powders result from subsequent non-isothermal annealing above 750 °C. The wet-milling route prevents detrimental oxidation, powder losses or severe contamination from the grinding media. It thus appears that milder MA processing followed by non-isothermal annealing at moderate-to-low heating rates are effective in providing single-phase iQC powders. Sintering by FAST results in homogeneous bulk solids with uniform ultrafine microstructure, which points out the absence of thermal field or chemical gradients during FAST. The electric field/pulsed current application promotes rapid neck-formation and densification without grain-growth. An important observation is that densification seemingly occurs mainly during the initial heating of the specimen. Detrimental effects such as microstructure coarsening or abnormal grain-growth caused by prolonged exposure to elevated temperatures could then be avoided by choosing a shorter dwell time at the sintering temperature.

Icosahedral ψ and bcc β-phases were found to form throughout the volume of the sintered parts. The β-phase has local atomic arrangements similar to the iQC ψ-phase [2,6]. Its formation has no dramatic effects upon the Al–Cu–Fe alloy performance in most applications [1–5,10]. Further studies are presently underway to clarify the formation of the β-phase during FAST and whether or not the same phase sequence develops as in non-isothermal annealing. It was recently demonstrated that carbon contamination from the graphite dies may safely be ruled out [16]. The variation of the heating rate merely causes a moderate shift of the transition temperatures, but does not modify the observed evolution of constituent phases with temperature. Hydrostatic pressure was also shown to have no influence on the phase transformation sequence [12]. The modest pressure application during heating in FAST is thus expected to have no effect. We have recently suggested [12] that rapid quenching under pressure may provide an efficient route to stabilize the QC ψ-phase against its competing crystalline phases. Further experimental work is however still needed to clarify this issue.

Acknowledgements

This work was supported by the European Marie Curie Programme (HPMD-CT-2001-00089) and by a DAAD-NSF collaborative grant.

References

[1] E. Huttunen-Saarivirta, J. Alloys Compd. 363 (2004) 150–174.

[2] H.-R. Trebin (Ed.), Quasicrystals, Wiley-VCH, Weinheim, 2003.

[3] S.M. Lee, E. Fleury, J.S. Kim, Y.C. Kim, D.H. Kim, W.T. Kim, H.S. Ahn, Mater. Res. Soc. MRS 643 (2001) K15.2.1–K15.2.12.

[4] B.C. Anderson, P.D. Bloom, K.G. Baikerikar, V.V. Sheares, S.K. Mallapragada, Biomaterials 23 (2002) 1761–1768.

[5] M. Yoshimura, A.P. Tsai, J. Alloys. Compd. 342 (2002) 451–454.

[6] R. Lück, L. Zhang, in Ref. [2], 2003, 26–44.

[7] V.V. Tcherdyntsev, S.D. Kaloshkin, A.I. Salimon, E.A. Leonova, I.A. Tomilin, J. Eckert, F. Schurack, V.D. Rogozin, S.P. Pisarev, Yu.P. Trykov, Mater. Manufact. Proc. 17 (2002) 825–841.

[8] B.S. Murty, P. Barua, V. Srinivas, J. Eckert, J. Non-Cryst. Solids 334–335 (2004) 44–47.

[9] X. Yong, I.T. Chang, I.P. Jones, J. Alloys Compd. 387 (2005) 128–133.

[10] F. Schurack, J. Eckert, L. Schulz, in: H.-R. Trebin (Ed.), Quasicrystals, Wiley-VCH, Weinheim, 2003, pp. 551–569.

[11] E. Fleury, J.H. Lee, S.H. Kim, G.S. Song, J.S. Kim, W.T. Kim, D.H. Kim, Mater. Res. Soc. MRS 643 (2001) K2.1.1–K2.1.6.

[12] F. Turquier, V.D. Cojocaru, M. Stir, R. Nicula, C. Lathe, E. Burkel, Rev. Adv. Mater. Sci. 8 (2004) 147–151.

[13] M. Knapp, C. Bähtz, H. Ehrenberg, H. Fuess, J. Sync. Rad. 11 (2004) 328–334.

[14] Z. Shen, Z. Zhao, H. Peng, M. Nygren, Nature 417 (2002) 266–269.

[15] J.R. Groza, in: C.C. Koch (Ed.), Nanostructured Materials, Noyes Publisher/William Andrew Publisher, New York, 2002, pp. 115–178.

[16] N. Bonasso, D. Rouxel, P. Pigeat, Mater. Sci. Eng. A 390 (2005) 166–170.